Research Square

Preprints are preliminary reports that have not undergone peer review.
They should not be considered conclusive, used to inform clinical practice,
or referenced by the media as validated information.

Platelet-derived microparticles induce CD8$^+$ T cell senescence in end-stage renal disease via the transfer of microRNA-550a-5p

Jinghong Zhao

zhaojh@tmmu.edu.cn

Xinqiao Hospital, Army Medical University (Third Military Medical University) https://orcid.org/0000-0001-9750-3285

Yuewen Sun

Xinqiao Hospital, Army Medical University (Third Military Medical University)

Qigang Lan

Xinqiao Hospital, Army Medical University (Third Military Medical University)

Yaqin Wang

Xinqiao Hospital, Army Medical University (Third Military Medical University)

Minhua Xie

Xinqiao Hospital, Army Medical University (Third Military Medical University)

Xinyi Wu

Xinqiao Hospital, Army Medical University (Third Military Medical University)

Liangjing Lv

Xinqiao Hospital, Army Medical University (Third Military Medical University)

Qin Xin

Xinqiao Hospital, Army Medical University (Third Military Medical University)

Jun Chen

College of Preventive Medicine, Army Medical University (Third Military Medical University)

Xiaoyi Zhong

Xinqiao Hospital, Army Medical University (Third Military Medical University)

Mengying Yao

Army Medical University (Third Military Medical University)

Shuiqing Gong

Army Medical University (Third Military Medical University)

Siyan Zhou

Xinqiao Hospital, Army Medical University (Third Military Medical University)

Junping Wang

Army Medical University https://orcid.org/0000-0001-5905-0940

Article

Keywords: End-stage renal disease, CD8+ T cells, cellular senescence, platelets, miR-550a-5p, PMPCB

Posted Date: January 27th, 2026

DOI: https://doi.org/10.21203/rs.3.rs-8468315/v1

License: This work is licensed under a Creative Commons Attribution 4.0 International License.
Read Full License

Additional Declarations: There is no conflict of interest

Version of Record: A version of this preprint was published at Experimental & Molecular Medicine on October 16th, 2026. See the published version at https://doi.org/10.1038/s12276-026-01876-z.

Abstract

Infection is a leading cause of high mortality in patients with chronic kidney disease (CKD), in which T cell dysfunction is considered as a typical feature in CKD patients. Although platelets are active participants in immune response, their role in regulating T cell function in CKD patients remains unclear. In this study, we demonstrate that $CD8^+$ T cell senescence may be a major contributor to the immunosuppressed state of end-stage renal disease (ESRD) patients, and that platelets derived from ESRD patients can induce premature $CD8^+$ T cell senescence, potentially through mediating mitochondrial dysfunction. Further investigations reveal that platelet-derived microparticles (PMPs) from ESRD patients promote $CD8^+$ T cell senescence via transferring miR-550a-5p, thereby decreasing PMPCB expression and inducing NDUFS8 cleavage failure. Finally, inhibition of miR-550a-5p and pretreatment with Nicotinamide Mononucleotide is capable of preventing platelet-induced $CD8^+$ T cell senescence in ESRD patients. Collectively, these findings suggest that the ectopic transient expression of platelet-derived miR-550a-5p in $CD8^+$ T cells promotes cellular senescence by regulating the PMPCB-NDUFS8 axis, which can be exploited to treat the ESRD-associated immunosenescence.

1. Introduction

Chronic kidney disease (CKD) has emerged as a critical global public health concern and is accompanied by a high incidence of multiple complications [1, 2]. It has been well recognized that infection is a leading cause of morbidity and mortality in patients with CKD, particularly those with end-stage renal disease (ESRD) [3]. Notably, the immunosuppressed state of CKD patients is characterized by dysfunction of innate and adaptive immune system, resulting in a proinflammatory milieu and a decreased cellular immunity [4]. Unfortunately, the understanding of the susceptibility to infection and immune dysfunction in CKD patients is still limited, and more effective measures are still needed in clinical practice.

The adaptive immune system possesses highly specific features in response to threats from pathogen and memory function [5]. T cells are the major cell components and responsible for mediating cell-based immune responses [6]. In CKD, there is a profound change in the total number and function of circulating T cells [7, 8]. Plenty of studies, including our own, have demonstrated a decrease in T cell number in CKD, as well as a concomitant increase in terminal differentiation and proinflammatory T cells [9, 10]. Furthermore, in the presence of numerous stimulations, such as uremia and dialysis, T cell replicative capacity is impaired, resulting in functional exhaustion and senescence [11, 12]. These two states share overlapping phenotypic and functional characteristics but differ in their distinct molecular and developmental signatures [13]. T cell exhaustion is marked by increased expression of a suite of inhibitory receptors, including programmed cell death protein 1 (PD-1) and cytotoxic T-lymphocyte antigen-4 (CTLA-4) [14], while T cell senescence is defined by features such as telomere shortening and loss of CD28, along with reciprocal expression of CD57 [15]. However, the underlying mechanisms by

which T cell exhaustion and senescence contribute to immune dysfunction upon ESRD remain largely unexplored.

Platelets, one of the most prevalent blood components, are well-known for their hemostatic and thrombotic functions. Interestingly, accumulating evidence now indicates that platelets also actively modulate immune responses [16, 17]. It is becoming increasingly clear that platelets can not only directly interact with immune cells by changing their surface expression of P-selectin or other receptors, such as Toll-like receptors, but also can release a number of granules and microparticles that regulate adaptive immunity [18]. Our findings have also revealed disrupted platelet homeostasis in the CKD milieu, with enhanced platelet-immune cell interactions and increased platelet-derived microparticles (PMPs) release [19, 20]. Given that plasma microparticles can alter T cell function and phenotype, and that PMPs are the most abundant microparticles present in the blood [21], it is important to improve our understanding of the role of platelet-T cell interactions in immune dysregulation upon ESRD.

In this study, we demonstrate that platelets from ESRD patients transfer miR-550a-5p through the release of PMPs, leading to miR-550a-5p ectopic expression in $CD8^+$ T cells, which induces mitochondrial dysfunction-mediated cellular senescence through negatively regulating peptidase-mitochondrial processing subunit beta (PMPCB) expression, culminating in cleavage failure of NADH: ubiquinone oxidoreductase core subunit S8 (NDUFS8) and a decrease in NAD + level. Importantly, inhibition of miR-550a-5p and supplement with Nicotinamide Mononucleotide (NMN) significantly attenuate mitochondrial dysfunction and cellular senescence of $CD8^+$ T cells. Hence, our findings uncover a novel platelet-$CD8^+$ T cell interaction and provided a promising strategy to prevent $CD8^+$ T cell senescence in ESRD.

2. Materials and Methods

2.1 Study Subjects

A total of 75 CKD patients in stages 3–5, who were not on dialysis and aged between 25 and 45 years, were enrolled from the Department of Nephrology at Xinqiao Hospital (Chongqing, China), and 45 healthy volunteers were recruited. All participants provided informed consent to take part in this study (Table S1). The study protocol was approved by the ethics committee of Xinqiao Hospital, Army Medical University (Institutional Review Board at No. 2025-267-01).

2.2 Animal Experiments

MiR-550a-5p agomir and negative control were synthesized by Biomics (The sequences listed in Table S2). Male C57BL/6J mice (8 weeks old) were purchased from Chongqing Tengxin Bioscience (Chongqing, China). Mice received tail vein intravenous injections of miR-550a-5p agomir or the negative control at a dose of 20 nmol once every four days for four weeks. All mice were euthanized 48 hours

after the final injection. All the experimental procedures were approved by the Animal Care and Use Committee of the Army Medical University (No. AMUWEC20255414).

2.3 Isolation of Human $CD8^+$ T cells and Platelets

Human whole blood was collected using sodium citrate anticoagulant. $CD8^+$ T cells were isolated using the ImunoSep Human $CD8^+$ T Cell Enrichment Kit (Precision Biomedicals, Shenzhen, China). The purity of the isolated $CD8^+$ T cells, assessed by flow cytometry, exceeded 95%. Purified cells were resuspended in RPMI 1640 medium (Meilunbio, Dalian, China) supplemented with 10% fetal bovine serum (Corning, NY, USA).

Platelet isolation was performed as previously described [20]. Briefly, blood was centrifuged at 160g for 15 minutes at room temperature. The upper two-thirds of the platelet-rich plasma (PRP) was collected and then recentrifuged at 160g for 10 minutes in the presence of 0.1 μg/mL prostacyclin. The resulting PRP was then centrifuged at 1000g for 10 minutes. The platelet pellet was resuspended in Tyrode's-HEPES buffer containing 10 μmol/L indomethacin and 0.1 μg/mL prostacyclin. Flow cytometric analysis of $CD45^+$ events confirmed that leukocyte contamination in the platelet suspension was less than 0.001%.

2.4 PMPs Isolation

PMPs were isolated as previously described [22]. Purified platelets were resuspended in saline with 1 mM calcium and 1 U/mL thrombin at 37°C for 60 minutes. Activation was terminated by adding EDTA to a final concentration of 20 mM, followed by centrifugation at 2000g for 20 minutes to remove platelets. The supernatants containing PMPs were centrifugated at 20,000g for 90 minutes at 4^oC, the pellet was collected for downstream analysis.

2.5 Co-culture

$CD8^+$ T cells co-cultured with platelets as previously described [16]. Purified $CD8^+$ T cells and platelets were co-cultured at a ratio of 1:450 in prepared RPMI 1640 medium. T cell activation was induced using coated anti-CD3 monoclonal antibody and soluble anti-CD28 monoclonal antibody (all Kxbiotech, beijing, China). Interleukin-2 (IL-2; Beyotime, Shanghai, China) was added to maintain cell expansion. Cells were cultured at 37oC in a humidified atmosphere containing 5% CO_2 for 7 days. According to the experimental design, $CD8^+$ T cells were harvested for subsequent analysis.

2.6 Flow Cytometry and Cell Sorting

Platelets were identified were identified based on scatter properties and $CD41^+$ PMPs were detected as particles < 1 μm in size and identified as $CD41^+$ and Annexin V^+ (Thermo Fisher Scientific) [19]. Platelet activation was assessed by measuring surface expression of P-selectin and activated integrin GPIIb/IIIa (both Thermo Fisher Scientific).

To determine T cell phenotype in peripheral blood, 100 μL of whole blood was processed to isolate peripheral blood mononuclear cells (PBMCs). For human T cells, PBMCs were stained with a lineage antibody cocktail comprising anti-CD3, anti-CD4, anti-CD8, anti-CD57, anti-PD-1, and anti-CD28 antibodies. For mouse T cells, a cocktail containing anti-CD3, anti-CD8, anti-CD44, and anti-CD153 antibodies was used.

To determine mitochondrial membrane potential, cells were incubated with 100 nM tetramethylrhodamine methyl ester (TMRM; Thermo Fisher Scientific) at 37^{o}C for 20 min. To determine reactive oxygen species (ROS) production, cells were incubated with 10 μM dichlorodihydrofluorescein diacetate (DCFH-DA; Sigma-Aldrich, St. Louis, MO, USA) at 37^{o}C for 30 min. Senescence-associated β-galactosidase (SA-β-Gal) activity was evaluated using the CellEvent™ Senescence Green Flow Cytometry Assay Kit (Thermo Fisher Scientific) according to the manufacturer's protocol.

To determine p21 and γ-H2A.X levels, cells were washed and fixed resuspended with 1 ml Foxp3 Fixation/Permeabilization working solution (Thermo Fisher Scientific) and incubated at room temperature for 30 min. Then, the cells were permeabilized with Permeabilization buffer (Thermo Fisher Scientific) in the presence of anti-phospho-H2A.X (Ser19) and anti-p21 at room temperature for another 30 min.

For mouse CD8^{+} T cells sorting, PMBCs were stained with indicative antibodies and isolated by fluorescence-activated cell sorting.

Cells were detected using a BD FACSverse flow cytometer (BD Biosciences) or sorted using a FACSAriaII (BD Biosciences). Data analysis was performed using FlowJo software (Tree Star Inc.).

2.7 Relative Telomere Length Measurement

To determine telomere length in CD8^{+} T cells, genomic DNA was extracted from isolated CD8^{+} T cells using the Fast DNA Extraction Kit (Bioroyee, Beijing, China) according to the manufacturer's protocol. Relative telomere length was determined using the Relative Telomere Length Quantification qPCR Assay Kit (ScienCell Research Laboratories, San Diego, CA, USA).

2.8 Cell Mito Stress Test

Oxygen consumption rate (OCR) was measured using the Seahorse XF HS Mini Analyzer (Agilent Technologies, Santa Clara, CA, USA). CD8^{+} T cells were seeded in XF8 cell culture microplates and analyzed with the Seahorse XFp Cell Mito Stress Test Kit (Agilent Technologies). Following three baseline respiration measurements without additives, sequential injections of mitochondrial modulators were performed: 1.5 μM oligomycin (ATP synthase inhibitor), by the addition of 2 μm FCCP and Rotenone & antimycin A (0.5 μm Rot/AA) for further measurements. OCR was expressed as units of picomoles (pmol) per minute, and data were normalized against the number of cells.

2.9 NAD+/NADH Assay

NAD+/NADH levels were quantified using the NAD+/NADH Assay Kit (LABLEAD, Beijing, China) according to the manufacturer's instructions. Concentrations were normalized to total protein content, expressed as μmol NAD+/NADH per mg protein. Relative NAD+/NADH levels were then analyzed and compared with control groups.

2.10 Cell Transfection

$CD8^+$ T cells were transfected with PMPCB overexpression plasmids (Youbio Biotechnology, Hunan, China), PMPCB-targeting siRNA or miR-550a-5p mimics/inhibitors (all from Biomics Biotechnologies, Jiangsu, China), using Lipofectamine 3000 (Thermo Fisher Scientific). Cells were harvested 48 hours post-transfection for downstream analysis (listed in Table S4, 5).

2.11 Construction of Reporter Plasmids and Dual Luciferase Reporter Analysis

A DNA fragment containing the predicted miR-550a-5p binding site within the 3' untranslated region (3' UTR) of human PMPCB was amplified from genomic DNA by PCR. The PCR product was cloned into the pmirGLO™ dual-luciferase vector (RabbitBio, Chengdu, China) and verified by Sanger sequencing. To assess binding specificity, site-directed mutagenesis was performed on the putative miR-550a-5p binding site (5'-CAGGCAC-3' → 5'-AGUUAGA-3') in the PMPCB 3' UTR. For luciferase assays, $CD8^+$ T cells were co-transfected with either pmirGLO-PMPCB-WT or pmirGLO-PMPCB-Mut, and miR-550a-5p mimic or negative control mimic (mimic-NC). Luciferase activity was measured 24 hours post-transfection using the Dual-Luciferase® Reporter Assay System (Promega, Madison, WI, USA). Firefly luciferase signals were normalized to Renilla luciferase activity for data analysis.

2.12 RNA Extraction and Quantitative real-time polymerase chain reaction (qPCR) Analysis

Total RNA was extracted from PMPs or $CD8^+$ T cells using TRIzol™ reagent (Thermo Fisher Scientific). Reverse transcription was performed using The RevertAid First Strand cDNA Synthesis Kit (MCE, Monmouth Junction, NJ, USA) for mRNA analysis or the microRNA (miRNA) 1st Strand cDNA Synthesis Kit (Vazyme, Nanjing, China) for miRNA analysis. qPCR was carried out using SYBR Green Master Mix (MCE) on a real-time PCR system. Small nuclear RNA U6 (RNU6) and β-actin served as endogenous controls for miRNA and mRNA quantification, respectively. Relative gene expression was calculated using the 2^(−ΔΔCt) method. Primer sequences are provided in Supplementary Table S6, 7.

2.13 MicroRNA Expression Profiling

Total RNA was isolated from PMPs obtained from five ESRD patients and five healthy controls using the TaKaRa RNAiso Plus reagent. The integrity and concentration of the extracted RNA were verified prior to library construction. Sequencing libraries were prepared and sequenced by BGI Genomics (Shenzhen, China) to generate miRNA expression profiles. Raw miRNA expression data were subjected to quantile normalization and $\log_2$ transformation. miRNAs with expression levels above the sample-specific

median were classified as highly expressed. Differential expression analysis identified miRNAs with > 1.2-fold upregulation or < 0.833-fold downregulation for subsequent bioinformatic investigation.

2.14 Western Blot

Mitochondria were isolated using a mitochondrial isolation kit (ACMEC, Shanghai, China). Proteins were extracted from the purified mitochondrial fraction using RIPA lysis (Beyotime) buffer supplemented with protease and phosphatase inhibitors. Protein expression levels were determined using anti-p21, anti-γ-H2A.X, anti-PMPCB, anti-NDUFS8, anti-β-actin, and anti-COX IV. Then, the membranes were incubated with appropriate secondary antibodies (all Abcam) for 1 h at 37°C and imaged by an Odyssey Infrared Imaging System (LI-COR Biosciences).

2.15 Immunofluorescence

$CD8^+$ T cells were fixed with 4% PFA, and blocked with 2% BSA. Cells were incubated overnight at 4°C with anti-p21, anti-γ-H2A.X, or anti-PMPCB, followed by FITC-conjugated secondary antibody (37°C, 1 h). Nuclei were stained with DAPI (Beyotime). Visualization was performed using a Zeiss LSM800 NLO confocal microscopy (Carl Zeiss).

2.16 Bioinformatics Analysis

The human PBMC single-cell RNA sequencing dataset (GSE233315) was obtained from the NCBI Gene Expression Omnibus (GEO) database. Data processing and analysis were performed using the Seurat R package (version 5.3.0). Quality control filtering was applied as follows: cells with gene counts between 500 and 4,000 were retained, UMI counts > 500 and < 15,000 were included; cells exhibiting high ambient RNA contamination (log10(genes per UMI) ≤ 0.8) were excluded; cells with mitochondrial gene content exceeding 10% were removed.

2.17 Statistical Analysis

Statistical analyses were performed using GraphPad Prism 9.0 (GraphPad Software). Data are presented as mean ± standard deviation (SD). The number of independent biological replicates (N) is specified in respective figure legends. Comparisons between two groups were analyzed using paired or unpaired two-tailed Student's t-tests, as appropriate. Comparisons among three or more groups were analyzed using one-way analysis of variance (ANOVA) followed by Tukey-Kramer post hoc tests. Associations between variables were assessed using Spearman's rank correlation coefficient. Statistical significance was defined as $p < 0.05$ for all analyses.

3. Results

3.1 Peripheral blood $CD8^+$ T cells develop premature senescence in ESRD patients

Initially, we re-analyzed a published single-cell RNA sequencing (scRNA-seq) data from PBMC obtained from healthy controls and ESRD patients (GSE233315). Interestingly, we found that the markers of T cell exhaustion, PDCD1 and CTLA-4 were comparable between healthy and ESRD patients, while Kyoto Encyclopedia of Genes and Genomes (KEGG) revealed a robust upregulated in cellular senescence score, particularly in $CD8^+$ T effector cells (Fig. 1a, b and S1a, b). Similarly, t-distributed Stochastic Neighbor Embedding (t-SNE) analysis by flow cytometry identified a mild increase in PD-1 in $CD4^+$ and $CD8^+$ T cells from patients with CKD stage 3–5 compared to healthy controls (Fig. 1c-e and S1c). Notably, CD57, a recognized marker used to identify terminally differentiated senescent T cells, and the proportion of $CD57^+$ cells within the $CD4^+$ T cell population showed no significant, while it was significantly higher within $CD8^+$ T cells of patients with CKD stage 3–5 (Fig. 1c-e and S1c). Furthermore, we found that $CD57^+CD8^+$ T cells were progressively developed along with advancing CKD and were most significant in ESRD (CKD stage 5) patients (Figure S1d). Besides, CD28 is an age-related immune biomarker, and the loss of CD28 coupled with the presence of CD57 ($CD28^-CD57^+$) constitutes a key hallmark of immunosenescence. Flow cytometry also demonstrated that the proportion of $CD28^-CD57^+$ cells was significantly increased within the $CD8^+$ T cell compartment of ESRD patients, whereas no significant difference in their proportion within $CD4^+$ T cells (Fig. 1f, g). Taken together, these data indicate that the T cell immune incompetence develops in the pathophysiological context of ESRD due to multifaceted dysregulation, and that premature $CD8^+$ T cell senescence potentially serving as a central contributor.

3.2 $CD8^+$ T cells exhibit upregulated senescence biomarkers accompanied with mitochondrial dysfunction in ESRD

Cellular senescence is defined as the irreversible loss of replicative potential caused by persistent DNA damage, accompanied by increased β-galactosidase activity, cell cycle arrest and telomere shortening [15]. Indeed, we observed significantly elevated expression of the DNA damage marker γ-H2A.X and the cyclin-dependent kinase inhibitor p21 in $CD8^+$ T cells from ESRD patients compared with healthy controls (Fig. 2a-c and S2a, b), as well as significantly increased SA-β-Gal activity and expression of the senescent proinflammatory cytokines tumor necrosis factor-α (TNF-α) and interferon-gamma (IFN-γ) (Fig. 2d, e). Meanwhile, relative telomere length analysis revealed progressive age-dependent telomere shortening in $CD8^+$ T cells in both groups, with significantly shorter telomeres observed in ESRD patients (Fig. 2f). Furthermore, senescence-associated mitochondrial dysfunction is considered an essential component of the senescent phenotype [23]. Accordingly, we detected a decrease in OCR, maximal respiratory capacity and Adenosine triphosphate (ATP) production (Fig. 2g). Mitochondrial dysfunction was further confirmed by the loss of mitochondrial membrane potential (Fig. 2h). Mitochondria are sensitive to oxidative stress, which is the most prominent characteristic of the CKD milieu, and we also observed ROS overproduction in $CD8^+$ T cells of ESRD patients (Fig. 2i). Collectively, these findings

demonstrate that CD8+ T cells from ESRD patients exhibit a comprehensive senescent phenotype characterized by well-established senescence markers and severe mitochondrial dysfunction.

3.3 Platelets from ESRD patients induce premature CD8+ T cell senescence of by mediating mitochondrial dysfunction

We next sought to identify the role of platelets from ESRD patients in premature CD8+ T cell senescence. We first established a co-culture system in which platelets derived from healthy donors or ESRD patients respectively were co-cultured with CD8+ T cells derived from healthy donors (Fig. 3a). As shown, CD8+ T cells cultured alone or co-cultured with platelets derived from healthy individuals did not show a cellular senescence phenotype over time (Fig. 3b-e). However, CD8+ T cells co-cultured with platelets derived from ESRD patient exhibited a dramatic acceleration of premature CD8+ T cell senescence by day 5, as evidenced by the upregulation of γ-H2A.X, p21, SA-β-Gal and CD57 (Fig. 3b, c). Besides, upregulation of senescent proinflammatory cytokines and shortened telomeres were also detected in CD8+ T cells after co-cultured with platelets from ESRD patients (Fig. 3d, e). Surprisingly, mitochondrial membrane potential decreased, impaired mitochondrial respiratory function and ROS overproduction were observed in CD8+ T cells at day 3 after co-cultured with platelets from ESRD patients, preceding the appearance of cellular senescence (Fig. 3f-h). In contrast, pretreatment with N-acetylcysteine (NAC), an antioxidant agent, effectively prevented mitochondrial dysfunction and cellular senescence in CD8+ T cells induced by platelets from ESRD patients (Figure S3), indicating that platelets from ESRD patients might be involved in the initiation of premature CD8+ T cell senescence through mediating mitochondrial dysfunction.

3.4 PMPs from ESRD patients mediate mitochondrial dysfunction and cellular senescence in CD8+ T cells

Previously, we have shown that CKD promotes platelet hyperreactivity, inducing the large-scale release of PMPs, which have been reported to mediate mitochondrial dysfunction [19, 24]. Consistently, remarkably increased platelet activity including P-selectin, activated GPIIb/IIIa expression, and PMPs release were verified in ESRD patients (Figure S4a, b). Notably, PMPs release in the peripheral blood of ESRD patients was correlated positively with cellular senescence biomarkers and ROS levels in CD8+ T cells, whereas correlated negatively with mitochondrial membrane potential, hinting that PMPs release may facilitate mitochondrial dysfunction and cellular senescence of CD8+ T cells in ESRD milieu (Fig. 4a-f). To interrogate whether PMPs directly regulate premature CD8+ T cells senescence, CD8+ T cells were treated with PMPs *ex vivo* (Fig. 4g). Accordingly, Dio-labeled PMPs were successfully internalized by CD8+ T cells (Fig. 4g). PMPs from ESRD patients significantly induced CD8+ T cells to undergo mitochondrial dysfunction and cellular senescence, while NAC dramatically relieved these effects (Fig. 4h-l and S4c-l). Hence, these results demonstrate that a direct action of PMPs on premature CD8+ T cells senescence by inducing mitochondrial dysfunction.

3.5 PMPs promote premature $CD8^+$ T cell senescence in an miR-550a-5p dependent manner

PMPs are enriched in platelet microRNAs, which play an important role in regulating mitochondrial dysfunction and cellular senescence [25]. PMPs were isolated from healthy controls and ESRD patients for miRNA profile detection. There were profound differences in PMP expression between healthy controls and ESRD patients, with 109 miRNAs upregulated and 57 miRNAs downregulated in ESRD-derived PMPs (Fig. 5a). Importantly, we identified that the greatest change in miRNA expression was miR-550a-5p, which was also confirmed to be the most remarkably upregulated (Fig. 5a, b). Unexpectedly, the Starbase, TargetScan and miRDB databases revealed that miR-550a-5p was not expressed in mice (data not shown). Interestingly, the miR-550a-5p content in $CD8^+$ T cells was much lower than in PMPs, while the miR-550a-5p content in in $CD8^+$ T cells of ESRD patients was higher than in healthy controls, suggesting that high levels of miR-550a-5p in ESRD-derived PMPs were transferred to $CD8^+$ T cells (Figure S5a). Similar results were also observed in $CD8^+$ T cells and platelets co-cultured system (Fig. 5c). To investigate the miR-550a-5p's role in mediating mitochondrial dysfunction and cellular senescence in $CD8^+$ T cells, we transfected the cells with miR-550a-5p mimic, which was verified by qPCR and immunofluorescence (Figure S5b, c). Following 48 hours of transfection, we observed that overexpression of miR-550a-5p induced a markedly elevated levels of cellular senescence and mitochondrial dysfunction biomarkers (Fig. 5d-j and S5d), as well as increased senescent proinflammatory cytokines expression and shortened telomeres (Fig. 5k, l). Conversely, treatment $CD8^+$ T cells with miR-550a-5p inhibitor significantly rescued platelets from ESRD patients-induced these effects under co-cultured system (Figure S6). Collectively, these results demonstrate platelets from ESRD patients-derived PMPs induce $CD8^+$ T cell senescence via miR-550a-5p-mediating mitochondrial dysfunction axis.

3.6 MiR-550a-5p induce mitochondrial dysfunction and cellular senescence in $CD8^+$ T cells via targeting PMPCB

To investigate the underlying mechanisms by which miR-550a-5p regulates $CD8^+$ T cells mitochondrial dysfunction-induced cellular senescence, bioinformatic analysis predicted 19 potential target mitochondrial genes of miR-550a-5p based on TargetScan, miRDB and MitoCarta 3.0 databases (Fig. 6a, Table S8). Gene Ontology (GO) enrichment analysis showed that the mitochondrial genes were markedly enriched in mitochondrial protein transport (Fig. 6b), suggesting that miR-550a-5p may induce mitochondrial dysfunction through mediating mitochondrial transport process disorders. Of note, considering that miRNAs negatively regulate gene expression at the post-transcriptional level [26]. we observed that PMPCB expression was significantly decreased at both mRNA and protein levels in $CD8^+$ T cells of ESRD patients (Figure S7a-c). PMPCB as the catalytic subunit of mitochondrial processing peptidase, which promotes the maturation of precursor proteins transported to mitochondria [27].

Besides, we detected that co-cultured with platelets from ESRD patients can reduce PMPCB expression in $CD8^+$ T cells (Fig. 6c, D and S7d). Similar results were observed in $CD8^+$ T cells when transfected with miR-550a-5p mimic (Figure S7e, f). Furthermore, bioinformatic analysis predicted perfect complementary sequences between miR-550a-5p and the PMPCB 3'-untranslated region (UTR) (Fig. 6e). Dual-luciferase reporter assays were conducted to identify the targeting efficacy of miR-550a-5p on PMPCB. Overexpression of miR-550a-5p markedly decreased luciferase activity, while no effect was detected on PMPCB 3'-UTR mutant luciferase reporter (Fig. 6f). Interestingly, interrogation of sequences in the 3'UTR of mouse PMPCB gene also identified a miR-550a-5p binding site (Figure S7g). Moreover, we treated mice with miR-550a-5p modified oligonucleotides (agomir). Analogous to human $CD8^+$ T cells, cellular senescence, mitochondrial dysfunction and PMPCB downregulation were also detected in $CD8^+$ T cells of mice treated with miR-550a-5p agomir (Figure S7h, Figure S8). Above all, these results demonstrate that miR-550a-5p could directly bind and downregulate PMPCB expression.

To determine the role of PMPCB in mitochondrial dysfunction and cellular senescence in $CD8^+$ T cells, we first transfected siRNA against PMPCB in $CD8^+$ T cells *ex vivo* (Fig. 7a). As expected, the absent of PMPCB induced decreased mitochondrial membrane potential and impaired mitochondrial respiratory, but increased ROS levels (Fig. 7b-d). Consistently, upregulation of cellular senescence biomarkers and pro-inflammation cytokines, as well as shortened telomeres were also observed in $CD8^+$ T cells with PMPCB knockdown, indicating its important role in maintaining mitochondrial homeostasis (Fig. 7e-k and S9a, b). On the contrary, overexpression of PMPCB significantly alleviated miR-550a-5p-induced mitochondrial dysfunction, ultimately mitigating cellular senescence in $CD8^+$ T cells (Figure S10). Taken together, these data underscore a critical role of miR-550a-5p in mediating premature $CD8^+$ T cell senescence by targeting PMPCB, which is essential for the maintenance of mitochondrial homeostasis.

3.7 NMN counteracts platelets from ESRD patients-induced and NDUFS8-mediated cellular senescence in $CD8^+$ T cells

To further elucidate PMPCB-mediated $CD8^+$ T cell senescence mechanisms, we identified six PMPCB-interacting proteins using a protein-protein interaction analysis (Fig. 8a). Notably, the nuclear-encoded NDUFS8 is a subunit of monitoring NADH dehydrogenase in mitochondrial complex I, which would be cleaved by mitochondrial processing peptides [28]. We found no significant difference in NDUFS8 expression in $CD8^+$ T cells between ESRD patients and healthy controls, as well as co-cultured with platelets from ESRD patients or treatment with the miR-550a-5p mimic in human and miR-550a-5p agomir in mouse $CD8^+$ T cells (Fig. 8b, c and S11a-d). Interestingly, we detected the precursor and mature forms of NDUFS8 in $CD8^+$ T cells of ESRD patients, while only mature form of NDUFS8 existed in $CD8^+$ T cells of healthy controls (Fig. 8b). Moreover, co-cultured with platelets of ESRD patients or treatment with miR-550a-5p mimic in human and miR-550a-5p agomir in mouse $CD8^+$ T cells induced cleavage failure of NDUFS8, while overexpression of PMPCB significantly alleviated these effects

(Fig. 8c and S11c, d). These results indicate the regulatory effect of PMPCB on the cleavage of NDUFS8. As reported, NDUFS8 suppression will impair electron transfer from NADH to ubiquinone, thereby decreasing NAD+/NADH ratio, which has been reported to drive cells into senescence [29, 30]. Indeed, ESRD patients exhibited decreased NAD + levels and NAD+/NADH ratios in $CD8^+$ T cells (Fig. 8d). Meanwhile, co-cultured with platelets of ESRD patients or treatment with miR-550a-5p mimic resulted in a similar reduction in NAD + levels and NAD+/NADH ratios, conversely, overexpression of PMPCB partially ameliorated this phenomenon (Fig. 8e and S11e). Therefore, we treated $CD8^+$ T cells with NMN, an intermediate in NAD + biosynthesis which plays a vital role in a variety of biological processes, and analyzed their mitochondrial function [31]. NMN treatment effectively attenuated mitochondrial dysfunction in $CD8^+$ T cells, thereby preventing platelets from ESRD patients-induced cellular senescence (Fig. 8f-j and S11f-i). Moreover, we performed an intraperitoneal injection of NMN (500 mg/kg per mouse) once every 3 days in miR-550a-5p agomir-treated mice for 4 weeks. Consistently, NMN treatment effectively alleviated mitochondrial dysfunction and cellular senescence in $CD8^+$ T cells of mice (Figure S12). Above all, these findings indicate that NMN may serve as a promising therapeutic drug for alleviating platelets from ESRD patients-mediated mitochondrial dysfunction and cellular senescence.

4. Discussion

Infection is a leading cause of morbidity and mortality in patients with CKD [3]. T cell activation significantly influences an individual's immune function and susceptibility to infection [6]. Although disturbances in T cell homeostasis in CKD have been extensively studied, significant knowledge gaps remain regarding the underlying mechanisms of T cell dysfunction [10]. In this study, we identify that premature $CD8^+$ T cell senescence is a key feature of altered T cell homeostasis in ESRD patients. We further demonstrate that platelets accelerate this senescence process by transferring PMPs containing miR-550a-5p into $CD8^+$ T cells, thereby downregulating PMPCB expression and inhibiting NDUFS8/NAD + axis. Conversely, inhibiting miR-550a-5p function or overexpressing PMPCB ameliorated platelet-induced premature $CD8^+$ T cell senescence in ESRD.

Patients with CKD are more prone to develop premature age-related diseases [11]. Immunosenescence contributes to the development of infections, cancers and autoimmune diseases, as well as accelerating the progression of fatal diseases, including cardiovascular and metabolic disorders, non-alcoholic fatty liver disease, and neurodegenerative diseases [32, 33]. However, the characteristics and molecular mechanisms underlying immune cell senescence in ESRD remain incompletely understood. In this study, integrated bioinformatic analysis and clinical sample validation revealed that $CD8^+$ T cells exhibit more pronounced senescent change characters compared to $CD4^+$ T cells, which is consistent with previous reports [9, 34]. Currently, the cause of T cell senescence in CKD is attributed to the chronic inflammation resulting from uremia or maintenance dialysis [11]. In our study, we enrolled patients who were not on dialysis, and observed that $CD8^+$ T cell senescence progressively developed along with advancing CKD.

Interestingly, we demonstrate that another factor, co-cultured with platelets from ESRD patients can induce $CD8^+$ T cell senescence, which cells derived from healthy controls. While the role of platelets in hemostasis is well known, they are also considered a cellular component of the innate immune system [17]. Based on our findings, we discovered that, in addition to uremia, platelets can serve as immune regulatory cells to mediate $CD8^+$ T cell senescence.

As known, platelets can directly interact with immune cells via specific receptors, such as CD41, CD42 and CD154, but our study excluded this effect using a flow cytometry gating strategy [17]. Besides, platelets can also release granules or microparticles to regulate innate and adaptive immunity. We also confirmed that increased PMP release in ESRD patients, and found that PMP levels correlated positively with $CD8^+$ T cell senescence. Of note, recently studies indicate that platelet-releasing particles are closely associated with cellular senescence, but their performance is inconsistent in different milieu [35, 36]. The release of platelet factor 4 by platelets in young mice alleviates cognitive impairment in older mice, while the release of miR-146 is upregulated in the hippocampus and frontal cortex of patients with Alzheimer disease. Given platelets have fully functional miRNA machinery, we isolated PMPs and performed a miRNA profiling to identify the leading cause of $CD8^+$ T cell senescence. Here, we detect that miR-550a-5p is the most significantly upregulated miRNA in PMPs of ESRD patients and that it accelerates $CD8^+$ T cell senescence. In addition, the upregulation of miR-550a-5p can also promote the proliferation and migration of cancer cells [37]. Taken together, it is plausible that miR-550a-5p may be implicated in proliferation and migration of cancer cells via mediating $CD8^+$ T cell senescence and immunosuppression. On the contrary, treating $CD8^+$ T cells with a miR-550a-5p inhibitor effectively attenuates cell senescence when co-cultured with platelets from ESRD patients. Interestingly, the aspirin, an antiplatelet agent, also exhibits anti-aging properties via antioxidant, proteostatic and immunometabolic mechanisms [38–40]. Hence, it is conceivable that antiplatelet may serve a promising strategy for alleviating $CD8^+$ T cell senescence.

Mitochondrial dysfunction and associated ROS production have also been found in aging and many aging-associated pathological conditions, whereas the impairment of mitochondrial function and morphology also govern the senescent phenotype [23]. In our study, we observe that, after co-cultured with platelets of ESRD patients, mitochondrial disorders in $CD8^+$ T cells preceded the appearance of senescence phenotypes, while NAC treatment significantly rescue these effects, indicating that platelets of ESRD may induce $CD8^+$ T cell senescence by mediating mitochondrial dysfunction. In order to characterize the molecular mechanisms by which miR-550a-5p regulates $CD8^+$ T cell senescence, we for the first time identify PMPCB as a target gene of miR-550a-5p using bioinformatics and dual luciferase reporter analyses. PMPCB is the catalytic subunit of the mitochondrial processing peptidase, which identifies and cleaves mitochondrial importing signals necessary for the proper transport of proteins into the mitochondria, and thus facilitates their maturation. A decrease or mutation in PMPCB levels would induce mitochondrial processing peptidase dysfunction, thereby accumulating the processing intermediates such as frataxin [41]. Meanwhile, PMPCB has been shown to play a key role in regulating

oxidant stress and apoptosis mediated by mitochondrial dysfunction [42, 43]. Here, knockdown of PMPCB in $CD8^+$ T cells exhibit similar effects, including decreased mitochondrial membrane potential, impaired mitochondrial respiratory function and increased ROS production. However, the specific mechanisms by which PMPCB deficiency induces mitochondrial dysfunction are not fully elucidated. Further investigations reveal that the decreased PMPCB impairs the maturation of the pro-NDUFS8 precursor protein, leading to a reduced NAD+/NADH ratio. NDUFS8 is a nuclear-encoded core subunit of human mitochondrial Complex I, and NDUFS8 deficiency displays an apparent reduction in NAD+/NADH ratio and a decrease in mitochondrial membrane potential [44]. Crucially, intracellular reduced NAD^+ levels are intimately linked to aging [45], while NMN treatment effectively attenuated mitochondrial dysfunction and cellular senescence in $CD8^+$ T cells. Hence, our findings suggest that therapeutic intervention of PMPCB-NDUFS8 axis opens new opportunities to promote $CD8^+$ T cell senescence and immune function.

In summary, these findings demonstrate that platelet-derived miR-550a-5p is responsible for $CD8^+$ T cell senescence via the PMPCB-NDUFS8 axis in ESRD. This study not only substantially advances our understanding of the immune-platelet interactions, but also provided a potential strategy to prevent premature $CD8^+$ T cell senescence upon ESRD.

Declarations

Data availability

Data from this study are available upon a reasonable request to the corresponding author.

Acknowledgments

The investigators thank all patients who participated in this study.

Funding

This study was supported by the Joint Funds of the National Natural Science Foundation of China (No. U22A20279), Key program of the Natural Science Foundation of China (Nos. 82530025 and 82030023), Chongqing Graduate Research and Innovation Project (No. CYB23281).

CRediT authorship contribution statement

Yuewen Sun: Investigation, Formal analysis, Writing – original draft. **Qigang Lan:** Conceptualization, Investigation, Formal analysis, Supervision, Writing – original draft, Writing – review & editing. **Yaqin Wang**: Investigation, Data curation. **Minhua Xie:** Investigation, Data curation. **Xinyi Wu:** Investigation, Data curation. **Liangjing Lv**: Investigation, Data curation. **Qin Xin:** Investigation, Data curation. **Jun Chen:** Investigation, Data curation. **Xiaoyi Zhong:** Investigation, Data curation. **Mengying Yao:** Investigation, Data curation. **Shuiqin Gong:** Investigation, Data curation. **Siyan Zhou:** Investigation, Data curation.

Junping Wang: Conceptualization, Supervision, Writing – review & editing. **Jinghong Zhao:** Conceptualization, Supervision, Writing – review & editing.

Declaration of competing interest

The authors declare that they have no known competing financial interests or personal relationships that could have appeared to influence the work reported in this paper.

Supplementary information

Supplementary information is available at (journal name)'s website

1. Supplemental Material

2. MicroRNA profile

References

1. Foreman KJ, Marquez N, Dolgert A, et al. Forecasting life expectancy, years of life lost, and all-cause and cause-specific mortality for 250 causes of death: reference and alternative scenarios for 2016-40 for 195 countries and territories. Lancet. 2018. 392(10159): 2052–2090.
2. Kovesdy CP. Epidemiology of chronic kidney disease: an update 2022. Kidney Int Suppl (2011). 2022. 12(1): 7–11.
3. Cheikh Hassan HI, Tang M, Djurdjev O, Langsford D, Sood MM, Levin A. Infection in advanced chronic kidney disease leads to increased risk of cardiovascular events, end-stage kidney disease and mortality. Kidney Int. 2016. 90(4): 897–904.
4. Kato S, Chmielewski M, Honda H, et al. Aspects of immune dysfunction in end-stage renal disease. Clin J Am Soc Nephrol. 2008. 3(5): 1526–33.
5. McComb S, Thiriot A, Akache B, Krishnan L, Stark F. Introduction to the Immune System. Methods Mol Biol. 2019. 2024: 1–24.
6. Buck MD, O'Sullivan D, Pearce EL. T cell metabolism drives immunity. J Exp Med. 2015. 212(9): 1345–60.
7. Lisowska KA, Storoniak H, Dębska-Ślizień A. T cell subpopulations and cytokine levels in hemodialysis patients. Hum Immunol. 2022. 83(2): 134–143.
8. Sampani E, Vagiotas L, Daikidou DV, et al. End stage renal disease has an early and continuous detrimental effect on regulatory T cells. Nephrology (Carlton). 2022. 27(3): 281–287.
9. Betjes MG, Langerak AW, van der Spek A, de Wit EA, Litjens NH. Premature aging of circulating T cells in patients with end-stage renal disease. Kidney Int. 2011. 80(2): 208–17.
10. Xiong J, Qiao Y, Yu Z, et al. T-Lymphocyte Subsets Alteration, Infection and Renal Outcome in Advanced Chronic Kidney Disease. Front Med (Lausanne). 2021. 8: 742419.

11. Crépin T, Legendre M, Carron C, et al. Uraemia-induced immune senescence and clinical outcomes in chronic kidney disease patients. Nephrol Dial Transplant. 2020. 35(4): 624–632.
12. Hartzell S, Bin S, Cantarelli C, et al. Kidney Failure Associates With T Cell Exhaustion and Imbalanced Follicular Helper T Cells. Front Immunol. 2020. 11: 583702.
13. Zhao J, Wang Z, Tian Y, Ning J, Ye H. T cell exhaustion and senescence for ovarian cancer immunotherapy. Semin Cancer Biol. 2024. 104–105: 1–15.
14. Zhao Y, Shao Q, Peng G. Exhaustion and senescence: two crucial dysfunctional states of T cells in the tumor microenvironment. Cell Mol Immunol. 2020. 17(1): 27–35.
15. Mittelbrunn M, Kroemer G. Hallmarks of T cell aging. Nat Immunol. 2021. 22(6): 687–698.
16. Zhu L, Huang Z, Stålesen R, Hansson GK, Li N. Platelets provoke distinct dynamics of immune responses by differentially regulating CD4 + T-cell proliferation. J Thromb Haemost. 2014. 12(7): 1156–65.
17. Koupenova M, Clancy L, Corkrey HA, Freedman JE. Circulating Platelets as Mediators of Immunity, Inflammation, and Thrombosis. Circ Res. 2018. 122(2): 337–351.
18. Dinkla S, van Cranenbroek B, van der Heijden WA, et al. Platelet microparticles inhibit IL-17 production by regulatory T cells through P-selectin. Blood. 2016. 127(16): 1976–86.
19. Yang K, Du C, Wang X, et al. Indoxyl sulfate induces platelet hyperactivity and contributes to chronic kidney disease-associated thrombosis in mice. Blood. 2017. 129(19): 2667–2679.
20. Lan Q, Du C, Xiong J, et al. Renal Klotho safeguards platelet lifespan in advanced chronic kidney disease through restraining Bcl-xL ubiquitination and degradation. J Thromb Haemost. 2022. 20(12): 2972–2987.
21. Neyrinck-Leglantier D, Tamagne M, Ben Rayana R, et al. Remodeling of immune system functions by extracellular vesicles. Front Immunol. 2025. 16: 1549107.
22. Qu M, Zou X, Fang F, et al. Platelet-derived microparticles enhance megakaryocyte differentiation and platelet generation via miR-1915-3p. Nat Commun. 2020. 11(1): 4964.
23. Miwa S, Kashyap S, Chini E, von Zglinicki T. Mitochondrial dysfunction in cell senescence and aging. J Clin Invest. 2022. 132(13).
24. Michael JV, Wurtzel J, Mao GF, et al. Platelet microparticles infiltrating solid tumors transfer miRNAs that suppress tumor growth. Blood. 2017. 130(5): 567–580.
25. Chen X, Luo Y, Zhu Q, et al. Small extracellular vesicles from young plasma reverse age-related functional declines by improving mitochondrial energy metabolism. Nat Aging. 2024. 4(6): 814–838.
26. Correia de Sousa M, Gjorgjieva M, Dolicka D, Sobolewski C, Foti M. Deciphering miRNAs' Action through miRNA Editing. Int J Mol Sci. 2019. 20(24).
27. Quirós PM, Langer T, López-Otín C. New roles for mitochondrial proteases in health, ageing and disease. Nat Rev Mol Cell Biol. 2015. 16(6): 345–59.
28. Lin BY, Zheng GT, Teng KW, et al. TAT-Conjugated NDUFS8 Can Be Transduced into Mitochondria in a Membrane-Potential-Independent Manner and Rescue Complex I Deficiency. Int J Mol Sci. 2021.

22(12).

29. Zhang H, Ryu D, Wu Y, et al. NAD+ repletion improves mitochondrial and stem cell function and enhances life span in mice. Science. 2016. 352(6292): 1436–43.
30. Wang S, Kang Y, Wang R, et al. Emerging Roles of NDUFS8 Located in Mitochondrial Complex I in Different Diseases. Molecules. 2022. 27(24).
31. Nadeeshani H, Li J, Ying T, Zhang B, Lu J. Nicotinamide mononucleotide (NMN) as an anti-aging health product - Promises and safety concerns. J Adv Res. 2022. 37: 267–278.
32. Furman D, Campisi J, Verdin E, et al. Chronic inflammation in the etiology of disease across the life span. Nat Med. 2019. 25(12): 1822–1832.
33. Guo L, Li X, Gould T, Wang ZY, Cao W. T cell aging and Alzheimer's disease. Front Immunol. 2023. 14: 1154699.
34. Iio K, Kabata D, Iio R, et al. Decreased thymic output predicts progression of chronic kidney disease. Immun Ageing. 2023. 20(1): 8.
35. Müller M, Kuiperij HB, Claassen JA, Küsters B, Verbeek MM. MicroRNAs in Alzheimer's disease: differential expression in hippocampus and cell-free cerebrospinal fluid. Neurobiol Aging. 2014. 35(1): 152–8.
36. Schroer AB, Ventura PB, Sucharov J, et al. Platelet factors attenuate inflammation and rescue cognition in ageing. Nature. 2023. 620(7976): 1071–1079.
37. Meng L, Chang S, Sang Y, et al. Circular RNA circCCDC85A inhibits breast cancer progression via acting as a miR-550a-5p sponge to enhance MOB1A expression. Breast Cancer Res. 2022. 24(1): 1.
38. Gao J, Liu Y, Si C, et al. Aspirin inhibits proteasomal degradation and promotes α-synuclein aggregate clearance through K63 ubiquitination. Nat Commun. 2025. 16(1): 1438.
39. Maria M, Bashir MH, Fares AE, AbuBakr N. The prophylactic anti-aging effect of aspirin (acetylsalicylic acid) on oxidative stress-induced damage in the buccal mucosa of D-galactose-induced aged rats. Sci Rep. 2025. 15(1): 13053.
40. Shi W, Lin H, Di W, He C, Shen Y. Granulosa cell RNA-Seq insights into senescence and sphingolipid metabolism disorder in PCOS: aspirin as a potential therapeutic drug. Reprod Biol Endocrinol. 2025. 23(1): 61.
41. Vögtle FN, Brändl B, Larson A, et al. Mutations in PMPCB Encoding the Catalytic Subunit of the Mitochondrial Presequence Protease Cause Neurodegeneration in Early Childhood. Am J Hum Genet. 2018. 102(4): 557–573.
42. Takai A, Dang H, Oishi N, et al. Genome-Wide RNAi Screen Identifies PMPCB as a Therapeutic Vulnerability in EpCAM + Hepatocellular Carcinoma. Cancer Res. 2019. 79(9): 2379–2391.
43. Zheng JF, He S, Zeng Z, Gu X, Cai L, Qi G. PMPCB Silencing Sensitizes HCC Tumor Cells to Sorafenib Therapy. Mol Ther. 2019. 27(10): 1784–1795.
44. Iannetti EF, Smeitink J, Willems P, Beyrath J, Koopman W. Rescue from galactose-induced death of Leigh Syndrome patient cells by pyruvate and NAD. Cell Death Dis. 2018. 9(11): 1135.

45. Chini C, Cordeiro HS, Tran N, Chini EN. NAD metabolism: Role in senescence regulation and aging. Aging Cell. 2024. 23(1): e13920.

Figures

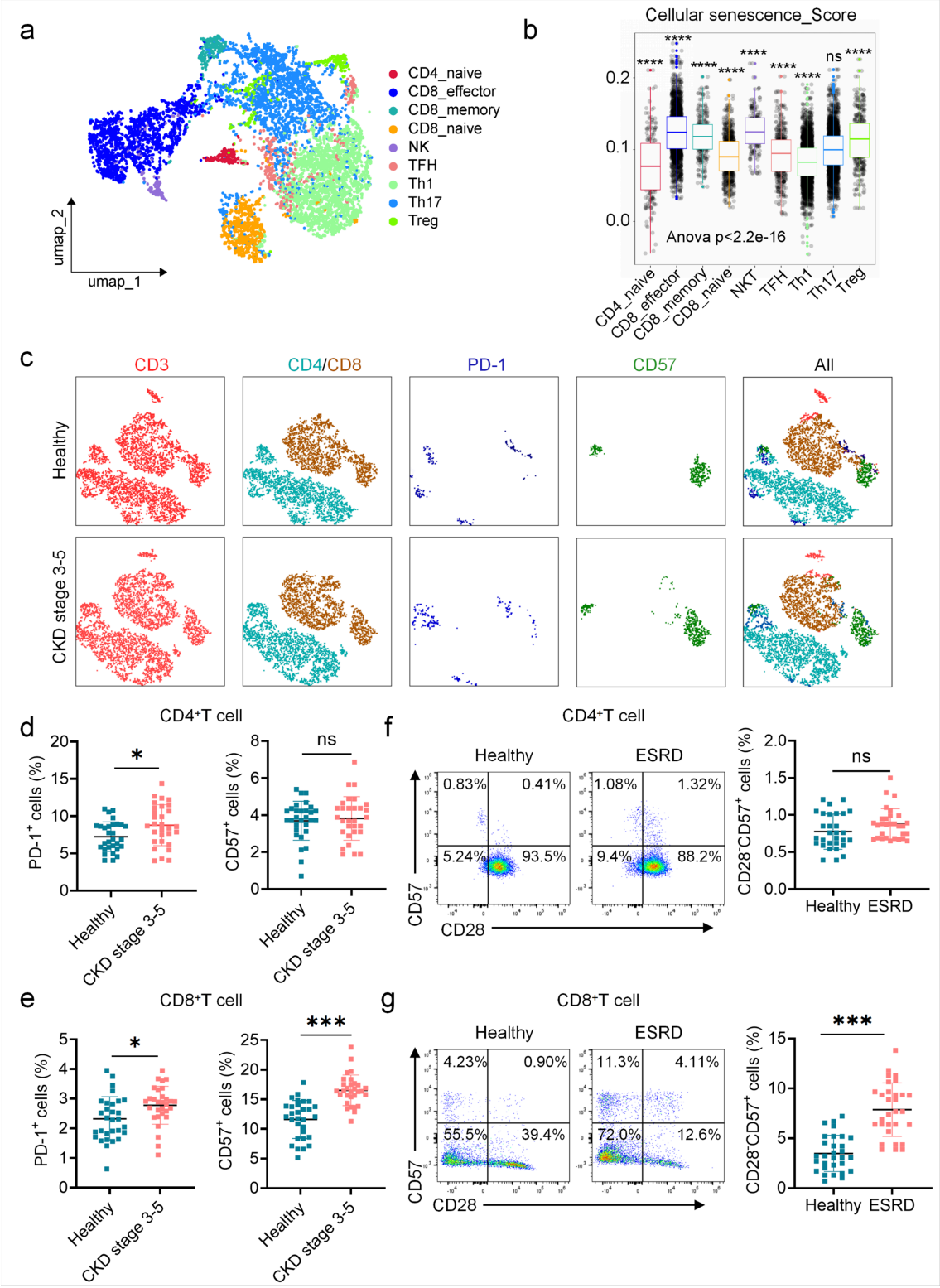


Figure 1

Peripheral blood $CD8^+$ T cells develop premature senescence in CKD patients. (a) t-SNE projection of PBMCs from healthy controls and ESRD patients, colored by major cell clusters identified through scRNA-seq analysis. Key T cell subsets and natural killer (NK) cells are indicated. TFH: T follicular helper cells. (b) Comparison of senescence scores across different T cell populations between the ESRD group and healthy group. (c) t-SNE plot of T cells overlaid with expression of indicated cell surface receptors determined by flow cytometry. (d, e) Quantitative analysis of the percentages of $PD\text{-}1^+$ cells and $CD57^+$ cells within $CD4^+$ and $CD8^+$ T cells between healthy controls and CKD patients (n = 30). (f, g) Representative flow cytometric analysis of the percentage of $CD28^-CD57^+$ cells within $CD4^+$ and $CD8^+$ T cells between healthy controls and ESRD patients (n = 30). Data are presented as mean ± SD and were analyzed by 2-tailed, unpaired Student's t-test. ns: no significance. *P < 0.05, ***P < 0.001.

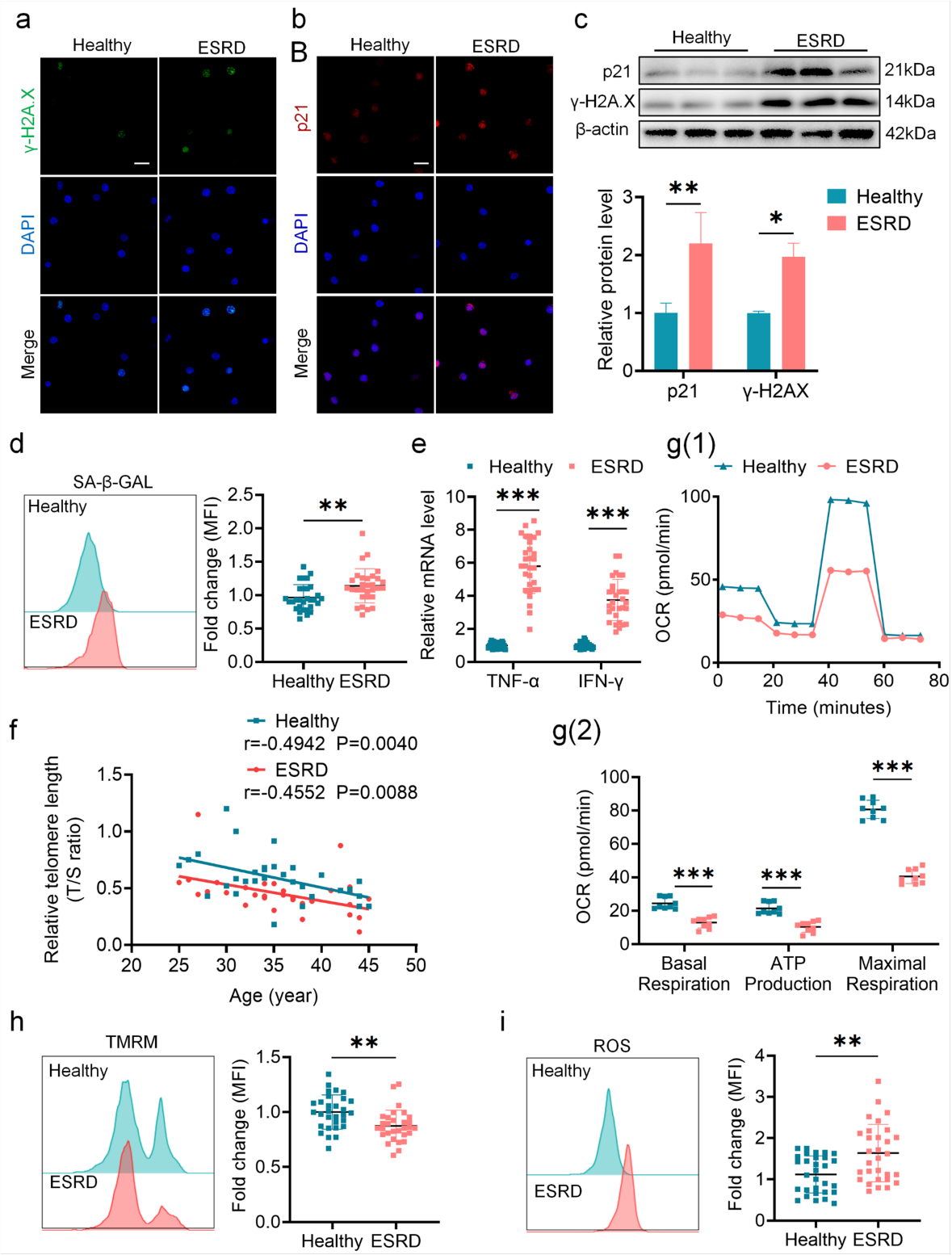


Figure 2

CD8⁺ T cells exhibit upregulated senescence biomarkers accompanied with mitochondrial dysfunction in ESRD. (a, b) Representative immunofluorescence staining images showing γ-H2A.X and p21 expression in CD8⁺ T cells of healthy controls and ESRD patients. Scale bar, 20 μm. (c) Western blot analysis of γ-H2A.X and p21 protein levels in CD8⁺ T cells of healthy controls and ESRD patients (n = 3). (d) Flow cytometric analysis of SA-β-GAL activity in CD8⁺ T cells of healthy controls and ESRD patients (n

= 30). (e) qPCR analysis of TNF-α and IFN-γ expression in CD8⁺ T cells of healthy controls and ESRD patients (n = 30). (f) Correlation analysis between relative telomere length and age in CD8⁺ T cells of healthy controls and ESRD patients (n = 30). (g) OCR in CD8⁺ T cells of healthy controls and ESRD patients and quantitation of basal respiration, ATP-linked respiration, and maximal respiration (n = 9). (h, i) Flow cytometric analysis of TMRM (h) and ROS (i) levels in CD8⁺ T cells of healthy controls and ESRD patients (n = 30). Data are presented as mean ± SD and were analyzed by 2-tailed, unpaired Student's t-test and Pearson's correlation analysis (F). *P < 0.05, **P < 0.01, ***P < 0.001.

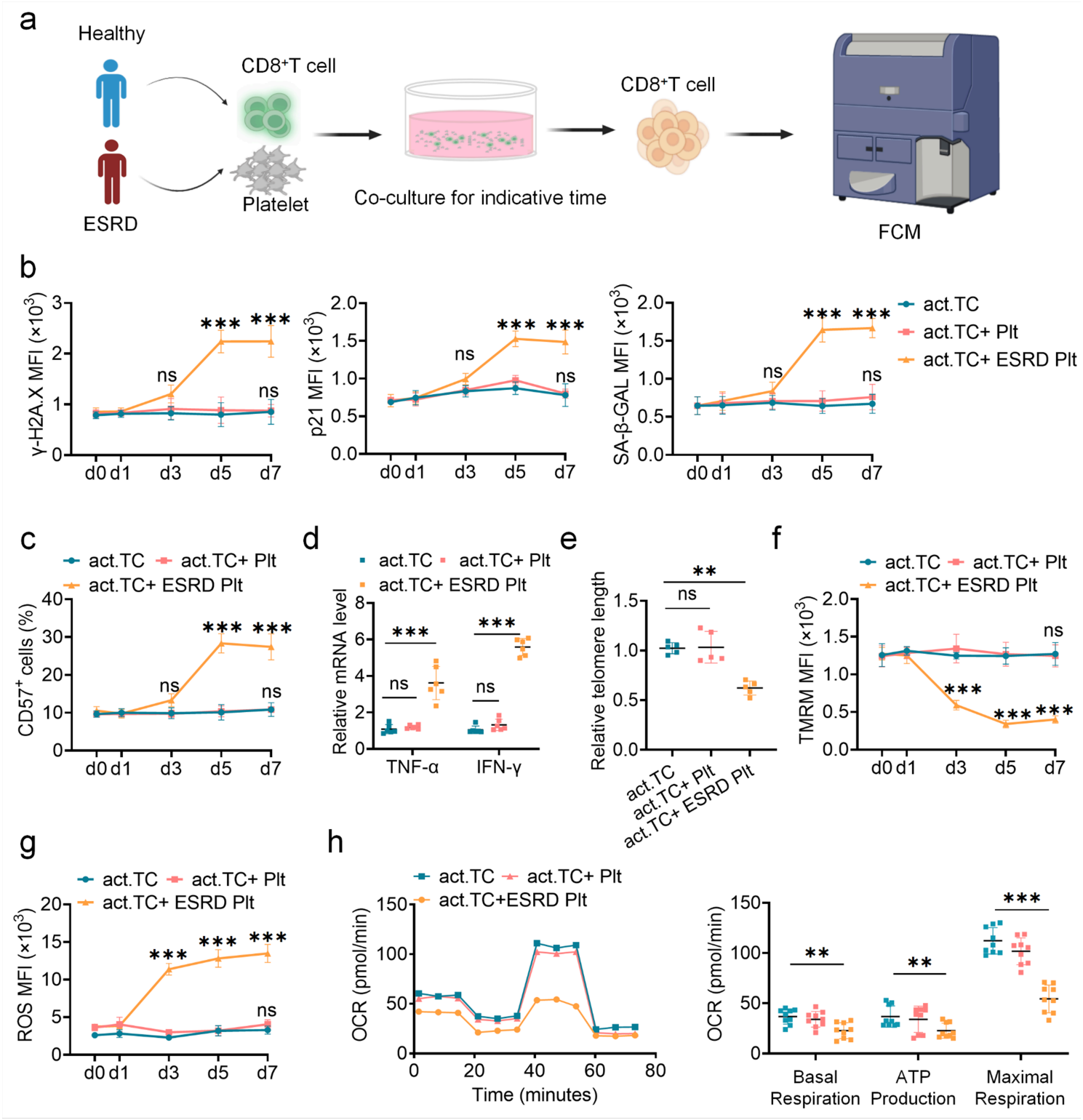


Figure 3

Platelets from ESRD patients induce premature $CD8^+$ T cell senescence of by mediating mitochondrial dysfunction. (a) Schematic diagram illustrating the co-culture system of platelets and $CD8^+$ T cells. (b) Flow cytometric analysis of γ-H2AX and p21 expression levels, and SA-β-Gal activity in $CD8^+$ T cells co-cultured with platelets from healthy controls or ESRD patients (n=3). (c) Flow cytometric analysis of the proportion of $CD57^+$ cells in $CD8^+$ T cells co-cultured with platelets from healthy controls or ESRD patients (n = 3). (d) qPCR analysis of TNF-α and IFN-γ expression in $CD8^+$ T cells from different groups (n = 6). (e) Relative telomere length in $CD8^+$ T cells from different groups (n = 6). (f, g) Flow cytometric analysis of TMRM (f) and ROS (g) levels in $CD8^+$ T cells across different groups (n = 3 for each analysis). (h) OCR in $CD8^+$ T cells from different groups, with quantitation of basal respiration, ATP production, and maximal respiration (n = 9). Data are presented as mean ± SD and were analyzed by one-way ANOVA. ns: no significance. **P < 0.01, ***P < 0.001.

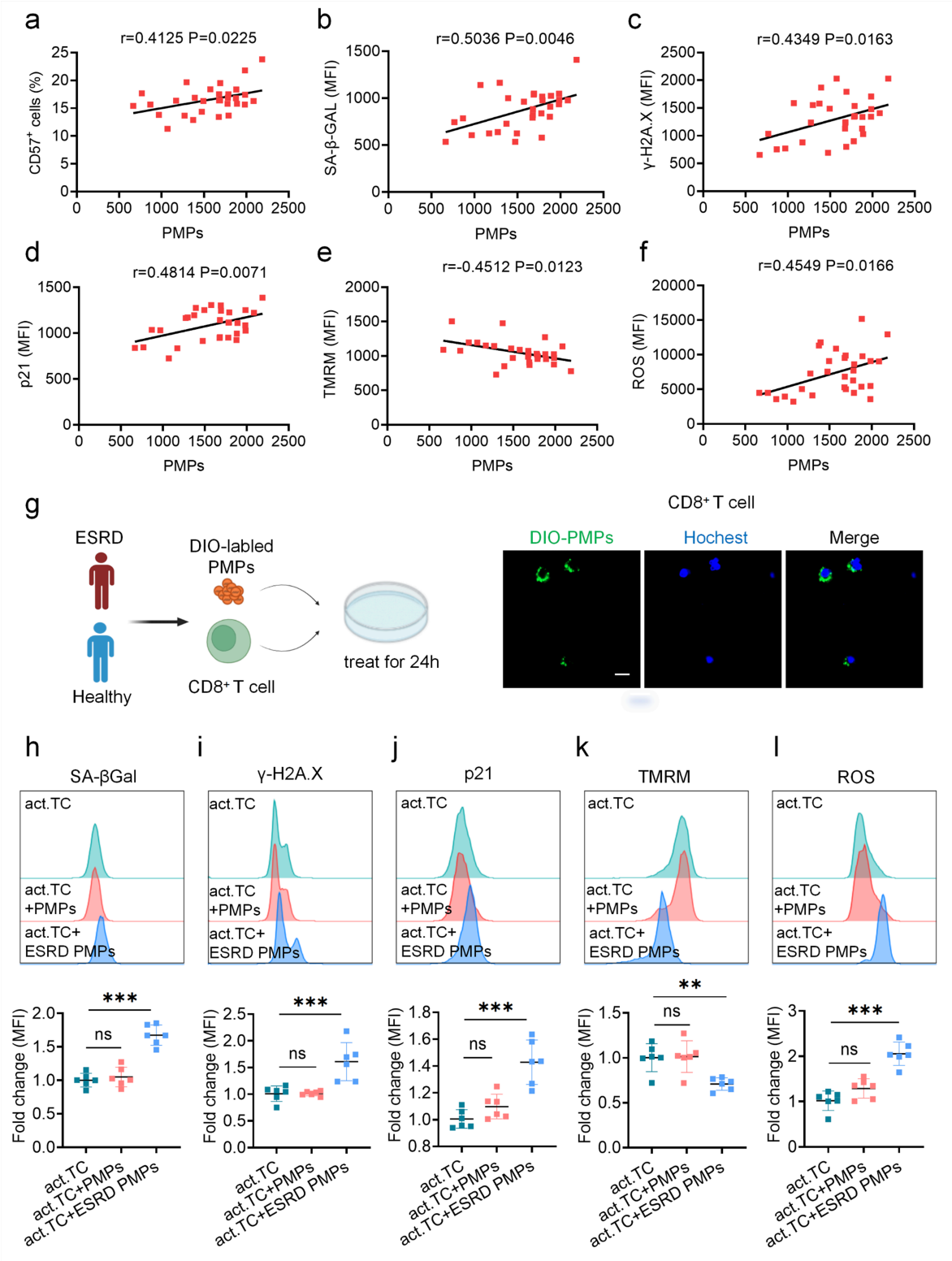


Figure 4

Platelets from ESRD patients-released MPs mediate mitochondrial dysfunction and cellular senescence in CD8⁺ T cells. (a–f) Correlation analysis between the levels of PMPs in peripheral blood and the proportion of CD57⁺ cells (a), SA-β-Gal activity (b), γ-H2AX level (c), p21 expression (d), TMRM levels (e), and ROS levels (f) in CD8⁺ T cells from ESRD patients (n = 30). (g) Schematic diagram and representative immunofluorescence images illustrating the internalization of PMPs by CD8⁺ T cells.

PMPs were labeled with DiO (green), and nuclei of CD8⁺ T cells were stained with Hoechst (blue). Scale bar, 20 μm. (h–l) Flow cytometric analysis of SA-β-Gal activity (h), γ-H2AX level (i), p21 expression (j), TMRM levels (k), and ROS levels (l) in CD8⁺ T cells treated with PMPs from healthy controls or ESRD patients (n = 6). Data are presented as mean ± SD and were analyzed by one-way ANOVA or Pearson's correlation analysis (a-f). **P < 0.01, ***P < 0.001.

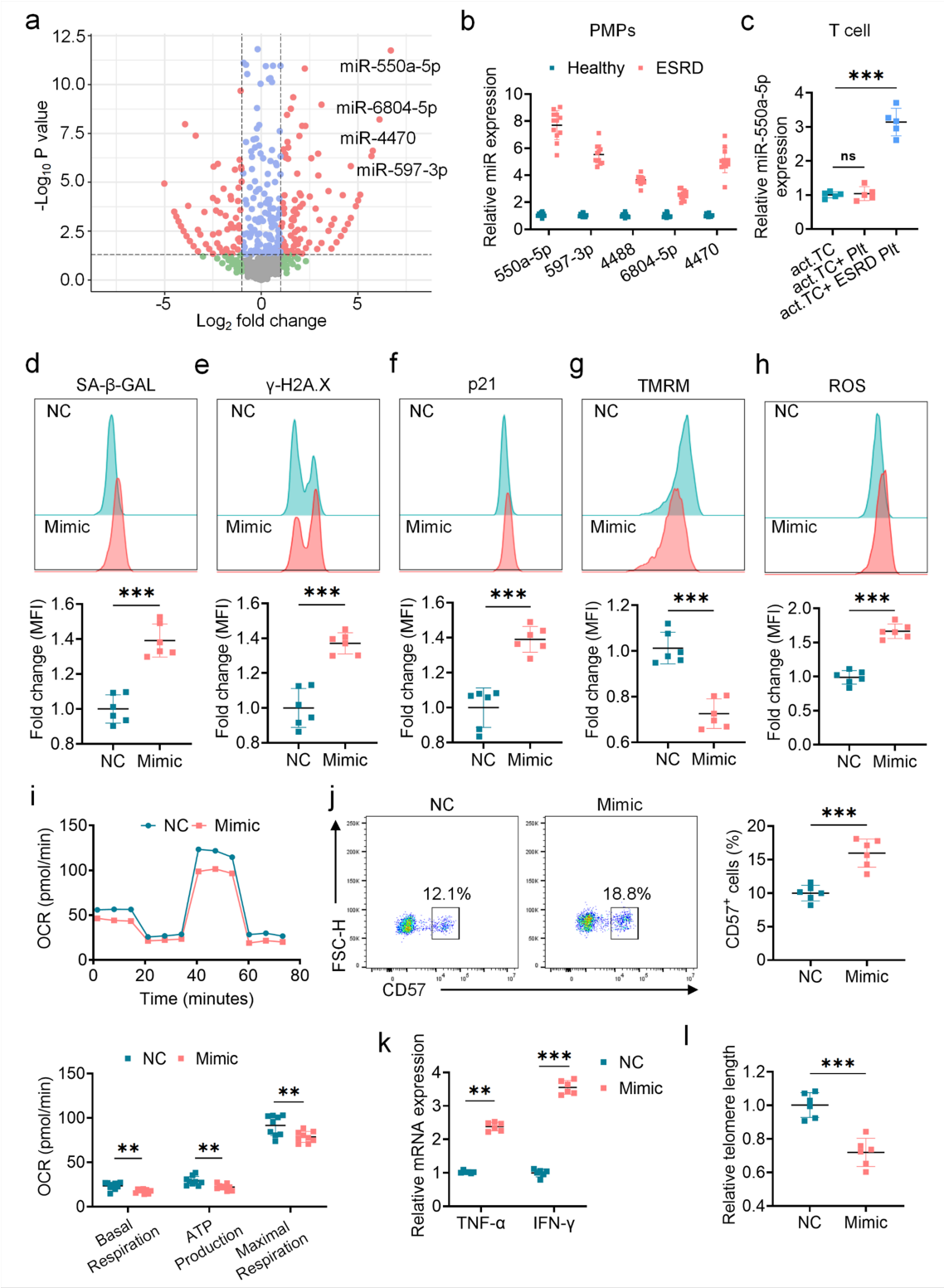


Figure 5

PMPs promote premature CD8$^+$ T cell senescence in an miR-550a-5p dependent manner. (a) Volcano plot illustrating differentially expressed miRNAs between healthy controls and ESRD patients, with thresholds set at $|\log_2(\text{fold change})| > 0.263$ (equivalent to >1.2 or <0.833-fold change) and $p<0.05$. (b) qPCR analysis of the expression of selected miRNAs in PMPs of healthy controls and ESRD patients (n = 12). (c) qPCR analysis of miR-550a-5p expression in CD8$^+$ T cells of healthy controls and ESRD patients (n = 6). (d-l) Flow cytometric analysis of SA-β-Gal activity (d), γ-H2AX level (e), p21 expression (f), TMRM levels (g), and ROS levels (h) in CD8$^+$ T cells treated with or without miR-550a-5p mimic (n = 6). (i) OCR in CD8$^+$T cells treated with or without miR-550a-5p mimic and quantitation of basal respiration, ATP production, and maximal respiration (n = 9). (j) Flow cytometric analysis the proportion of CD57$^+$ cells in CD8$^+$ T cells treated with or without miR-550a-5p mimic (n = 6). (k-l) qPCR analysis of TNF-α and IFN-γ expression (k) and relative telomere length (l) in CD8$^+$ T cells treated with or without miR-550a-5p mimic (n = 6). Data are presented as mean ± SD and were analyzed by 2-tailed, unpaired Student's t-test or one-way ANOVA (b, f). ns: no significance. **P < 0.01, ***P < 0.001.

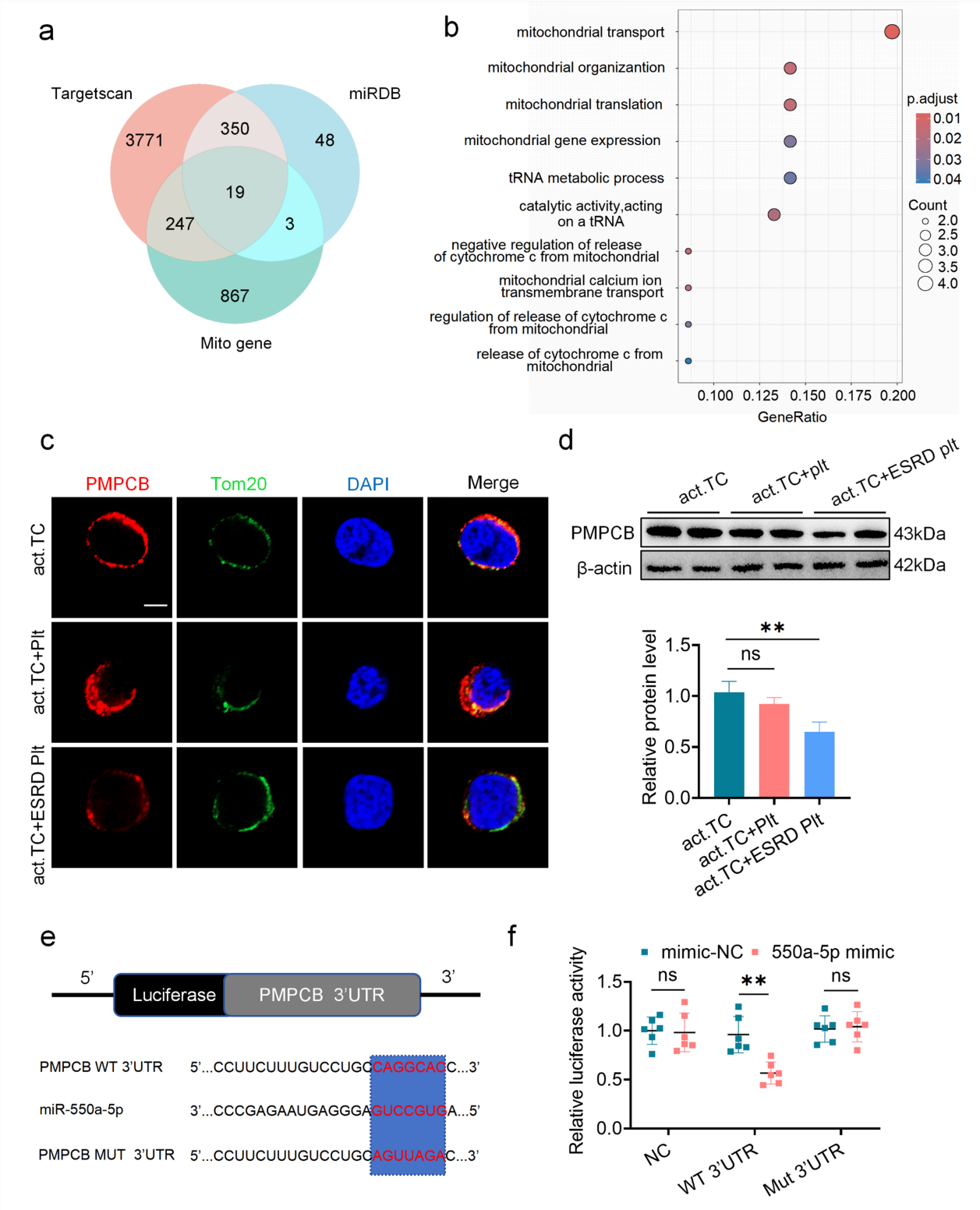


Figure 6

MiR-550a-5p regulates PMPCB expression via directly binding to its 3'UTR region. (a) Venn diagram showing the overlap between predicted target genes of miR-550a-5p from TargetScan and miRDB databases and human mitochondrial genes sourced from the MitoCarta database. (b) GO enrichment analysis of the predicted mitochondrial target genes. (c) Representative immunofluorescence staining images showing PMPCB expression (red) in CD8⁺ T cells co-cultured with platelets from healthy controls

or ESRD patients. Mitochondria were labeled with Tom20 (green). Scale bar, 10 μm. (d) Western blot analysis of PMPCB protein levels in $CD8^+$ T cells co-cultured with platelets from healthy controls or ESRD patients (n = 3). (e) Schematic illustration of the wild-type (WT) and mutant (Mut) putative miR-550a-5p binding sites within the 3' untranslated region (UTR) of the PMPCB gene cloned into a luciferase reporter vector. (f) Relative luciferase activity in $CD8^+$ T cells co-transfected with either the WT or Mut PMPCB 3' UTR reporter plasmid and miR-550a-5p mimic or negative control (NC) miRNA. Luciferase activity was normalized to Renilla luciferase activity (n = 6). Data are presented as mean ± SD and were analyzed by 2-tailed, unpaired Student's t-test or one-way ANOVA (D). ns: no significance. **P < 0.01.

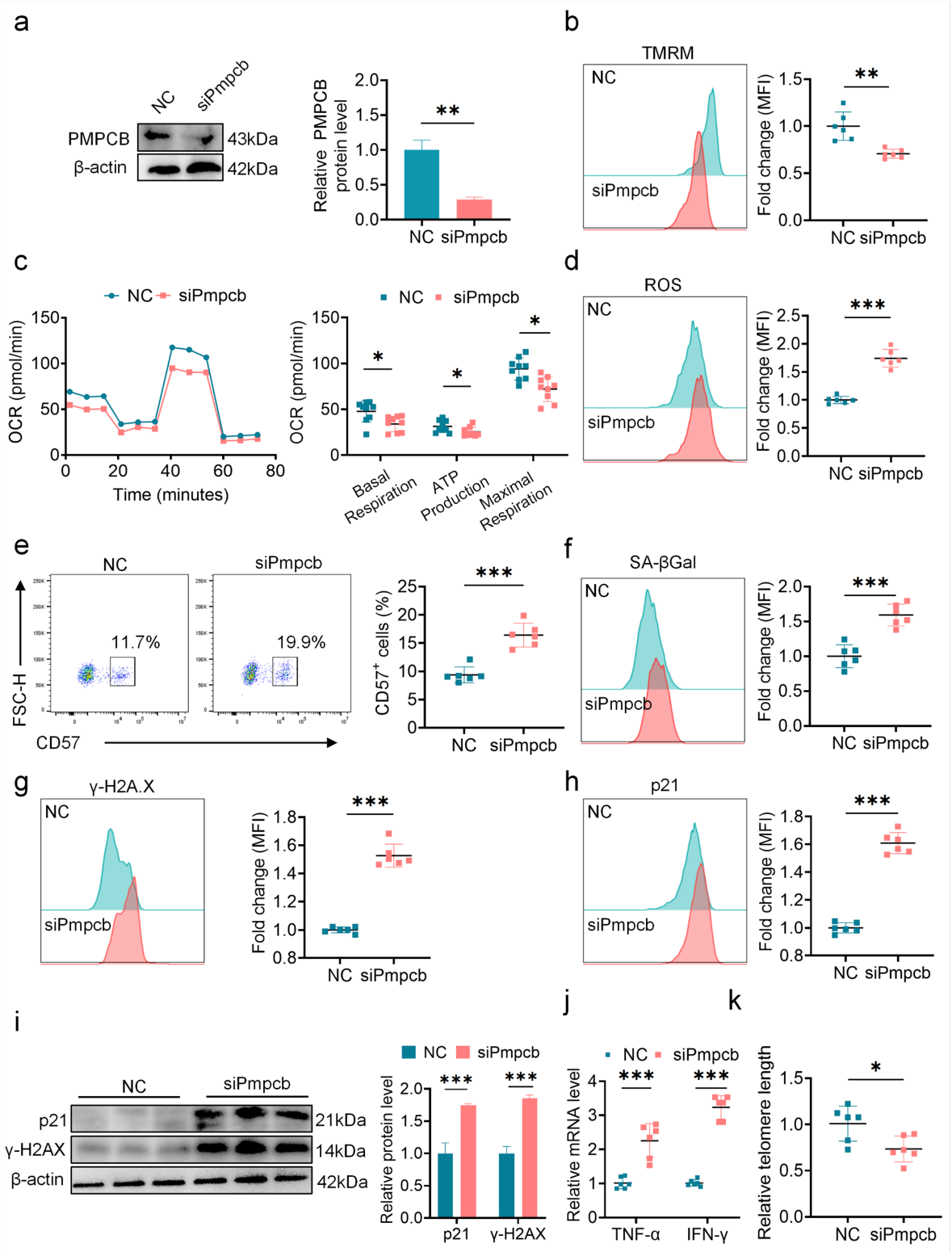


Figure 7

Knockdown of PMPCB induces mitochondrial dysfunction and cellular senescence in CD8⁺ T cells. (a) Western blot analysis of PMPCB protein levels in CD8⁺ T cells treated with PMPCB-specific siRNA or control siRNA (n = 3). (b) Flow cytometric analysis of TMRM levels in CD8⁺ T cells treated with PMPCB-specific siRNA or control siRNA (n = 6). (c) OCR in CD8⁺ T cells treated with PMPCB-specific siRNA or control siRNA, with quantitation of basal respiration, ATP production, and maximal respiration (n = 9).

(d–h) Flow cytometric analysis of reactive oxygen species (ROS) levels (d), proportion of CD57⁺ cells (e), SA-β-Gal activity (f), γ-H2AX level (g), and p21 expression (h) in CD8⁺ T cells treated with PMPCB-specific siRNA or control siRNA (n = 6). (i) Western blot analysis of γ-H2AX and p21 protein levels in CD8⁺ T cells treated with PMPCB-specific siRNA or control siRNA (n = 3). (j, k) qPCR analysis of TNF-α and IFN-γ expression (j) and relative telomere length (k) in CD8⁺ T cells treated with PMPCB-specific siRNA or control siRNA (n = 6). Data are presented as mean ± SD and were analyzed by 2-tailed, unpaired Student's t-test. ns: no significance. *P < 0.05, **P < 0.01, ***P < 0.001.

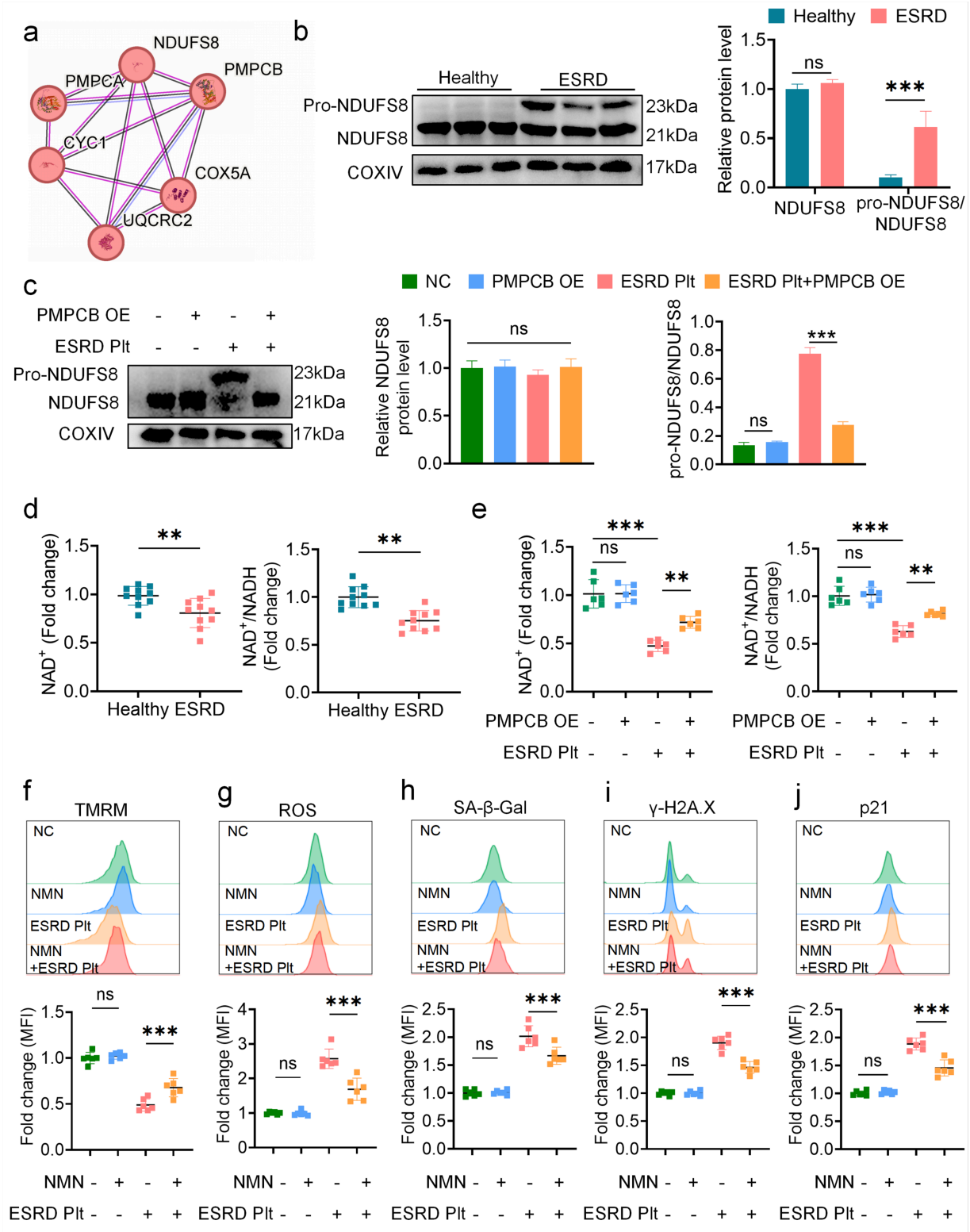


Figure 8

NMN counteracts platelets from ESRD patients-induced and NDUFS8-mediated cellular senescence in $CD8^+$ T cells. (a) Prediction of PMPCB-interacting proteins using the STRING database platform. (b) Western blot analysis of NDUFS8 expression in $CD8^+$ T cells of healthy controls and ESRD patients (n = 3). (c) Western blot analysis of NDUFS8 expression in $CD8^+$ T cells transfected with or without PMPCB overexpression plasmids under co-cultured system (n = 3). (d) Measurement of NAD^+ content and NAD^+/NADH ratio in $CD8^+$ T cells of healthy controls and ESRD patients (n = 10). (e) Measurement of NAD^+ content and NAD^+/NADH ratio in $CD8^+$ T cells transfected with or without PMPCB overexpression plasmids under co-cultured system (n = 6). (f-j) Flow cytometric analysis of TMRM levels (f), ROS levels (g), SA-β-Gal activity (h), γ-H2AX level (i), p21 expression (j) in $CD8^+$ T cells pretreated with or without 100 μM NMN under co-cultured system (n = 6). Data are presented as mean ± SD and were analyzed by 2-tailed, unpaired Student's t-test (b, d) or one-way ANOVA. ns: no significance. *P < 0.05, **P < 0.01, and ***P < 0.00

Supplementary Files

This is a list of supplementary files associated with this preprint. Click to download.

- GraphicalAbstract.jpg
- MicroRNAprofile.xls
- UneditedWBgel.pdf
- SupplementalMaterial.docx